The addition of calcium chloride in combination with a lower draining pH to change the microstructure and improve fat retention in Cheddar cheese

Lydia Ong[a, b, c], Kevany Soodam[a, b], Sandra E. Kentish[a, c], Ian B. Powell[d] and Sally L. Gras[a, b, c,*]

[a]Particulate Fluid Processing Centre, Department of Chemical and Biomolecular Engineering, The University of Melbourne, Parkville, Vic 3010, Australia.

[b]The Bio21 Molecular Science and Biotechnology Institute, The University of Melbourne, Parkville, Vic 3010, Australia.

[c]ARC Dairy Innovation Hub, Department of Chemical and Biomolecular Engineering, The University of Melbourne, Parkville, Vic 3010, Australia.

[d]Dairy Innovation Australia Limited, Werribee, Vic 3030, Australia.

*Corresponding author: sgras@unimelb.edu.au (S.L. Gras)

Tel.: +61-3-8344 6281; fax: +61-3-8344 4153

ABSTRACT

Calcium chloride addition and the whey draining pH are known to impact on cheese making. The effect of 100 or 300 mg kg^{-1} calcium chloride ($CaCl_2$) and the whey draining pH (6.2 and 6.0) on the microstructure of Cheddar cheese was assessed using confocal and cryo scanning electron microscopy. The gel made with 300 mg kg^{-1} $CaCl_2$ was found to have a denser protein network and smaller pores than the gel with lower or no $CaCl_2$ addition. $CaCl_2$ addition reduced fat lost to the sweet whey. The texture of the cheeses with a lower draining pH was harder and moisture content lower. Our results show that the combination of calcium addition and lower draining pH could be used to increase network formation at the early stages of cheese making to improve fat retention while maintaining a similar level of total calcium in the final cheese.

1. Introduction

Calcium chloride ($CaCl_2$) is added to cheese milk to assist milk gelation (Okigbo, Richardson, Brown & Ernstrom, 1985; Ustunol & Hicks, 1990), to improve the cheese making process (Gastaldi, Pellegrini, Lagaude & Fuente, 1994) and/or to increase cheese yield (Wolfschoon-Pombo, 1997). The effect of the concentration of calcium (Ca) on rennet induced coagulation has been reported in various studies (Dalgleish, 1983; Lucey & Fox, 1993; Udabage, McKinnon & Augustin, 2001; Zoon, van Vliet & Walstra, 1988) where a higher calcium concentration results in a faster rennet coagulation due to the combined effect of the increased calcium ion activity and a drop in milk pH, leading to changes in cheese properties (Ong, Dagastine, Kentish & Gras, 2013a).

The level of $CaCl_2$ added varies between manufacturers and regions. Typically, a concentration of 100-200 mg $CaCl_2$ kg^{-1} of milk is added (Gastaldi et al., 1994; Okigbo et al., 1985; Wolfschoon-Pombo, 1997), although this may reach up to 500 mg kg^{-1} in experimental studies (Ustunol & Hicks, 1990). The United States Federal standard limits the addition of $CaCl_2$ up to a level of 200 mg kg^{-1} (Federal Register, 1982), while other codes such as the Australian and New Zealand food standard or Codex Alimentarius do not specify limits. Addition of 200-300 mg kg^{-1} $CaCl_2$ has been shown to produce a denser gel network, which significantly increases the fat retained within the curd and decreases the fat lost to sweet whey (Ong et al., 2013a). More calcium is also present in the final cheese when more $CaCl_2$ is added to the milk. Increasing the concentration of calcium, however, may lead to undesirable properties such as the formation of calcium lactate crystals (CLC), a common defect in Cheddar cheese (Phadungath & Metzger, 2011).

The concentration of Ca in the final cheese can also affect the texture of the cheese immediately after pressing and during ripening. A higher level of total Ca increases cross-linking between casein micelles, leading to a harder gel (Choi, Horne, Johnson & Lucey, 2008). Conversely, the loss of insoluble Ca may increase repulsion between the exposed casein micelles phosphoserine residues resulting in a weaker gel network (Choi et al., 2008). The changes in gel properties may then in turn affect the textural properties of the cheese. Consequently, cheese with a low level of Ca, such as Cheshire cheese, tends to be crumbly, whereas cheese with high level of Ca, such as Gouda or Swiss, tends to be more rubbery and elastic (Lucey & Fox, 1993).

The draining pH is known to have a large influence on the mineral content of a cheese and decreases in draining pH can decrease the mineral content (Dalgleish & Law, 1989; Guinee, Feeney, Auty & Fox, 2002; Lucey & Fox, 1993). This change influences cheese texture and also the amount of lactose remaining in the curd and consequently the concentration of lactic acid and final pH, as well as the retention of some types of coagulant (e.g. retention of more chymosin at lower pH). This retention of rennet has implications for the proteolysis of cheese during maturation (Holmes, Duersch & Ernstrom, 1977). The analysis of mozzarella by scanning electron microscopy has shown that lowering the draining pH from 6.4 to 6.15 or to 5.9 resulted in an increase in the fusion of para-casein particles, producing a more continuous three dimensional network (Kiely, Kindstedt, Hendricks, Levis, Yun & Barbano, 1992). A lower whey draining pH in buffalo-milk mozzarella production (pH 5.3 vs pH 6.2) was also found to increase the yield of the cheese but the decrease in the level of total calcium adversely affected the melting properties of the cheese (Yazici & Akbulut, 2007).

The aim of this study was to investigate the effect of calcium chloride addition in combination with the lowering of the draining pH. Although the effect of $CaCl_2$ addition or draining pH has been well described for different cheeses, including Cheddar and Gouda cheese (Ong et al., 2013a; Walstra, Wouters & Geurts, 2006), the combination of these two processing parameters has not been investigated. These process adjustments may provide an approach to improve fat retention and cheese yield whilst reducing the concentration of calcium in the final cheese in order to avoid defect formation. The microstructure of the gel, cooked curd, milled curd and the final cheese were a specific focus of this work. Studies investigating the effect of draining pH on the microstructure of cheese are limited and have only focussed on mozzarella cheese to date (Kiely et al., 1992). This study uses the combination of confocal laser scanning microscopy (CLSM) and cryo scanning electron microscopy (cryo SEM) to examine the effect of calcium and draining pH. The composition and the texture of the cheese are also investigated.

2. Materials and methods

2.1. Cheese making

Six batches of Cheddar cheeses (Batches 1-6) were made in random order over three days at the Warrnambool Cheese and Butter pilot plant (WCB, Allansford, Australia) with different

86 levels of calcium chloride addition: 0 mg kg^{-1} cheese milk (Batch 1 control cheese and Batch 4),
87 100 mg kg^{-1} cheese milk (Batches 2 and 5) and 300 mg kg^{-1} cheese milk (Batches 3 and 6) and
88 different whey draining pH (Batches 1-3 drained at pH 6.2 and Batches 4-6 drained at pH 6.0).
89 Raw milk was standardized with cream and ultrafiltration retentate to obtain cheese milk with a
90 protein to fat ratio of 0.79. The cheese milk was then pasteurized at 72°C for 15 s and cooled to
91 32°C. The cheese milk was weighed (20 kg) and transferred to a cheese vat maintained at 32°C
92 before inoculation with 1.2 % (w/w) of mixed-strain *Lactococcus lactis* starter (Dairy Innovation
93 Australia, Werribee, Australia) cultured in bulk by WCB. The $CaCl_2$ (Ajax Finechem, Taren
94 Point, Australia) was added to Batches 2, 3, 5 and 6 immediately after starter addition. The total
95 calcium concentration of the cheese milk was 1125 ± 35 mg kg^{-1} (Batches 1 and 4), 1176 ± 35
96 mg kg^{-1} (Batches 2 and 5) and 1268 ± 36 mg kg^{-1} (Batches 3 and 6). The cheese-milk was stirred
97 at 20 revolutions per min (rpm) and ripened for 10-25 min (Table 1). The ripening time was
98 varied in order to achieve a similar pH at the point of rennet addition (~ pH 6.5). This is needed
99 due to the variation in the milk pH as a result of the addition of calcium chloride. The ripening
100 time of milk was shorter for samples with additional $CaCl_2$, as indicated in Table 1.
101 Rennet (Hannilase L; 690 IMCU mL^{-1}, Chr. Hansen, Bayswater, Australia) was added at
102 a concentration of 0.06 mL kg^{-1} for all batches. The coagulated cheese-milk was then cut. The
103 total coagulation time, defined here as time from rennet addition to cutting, varied between
104 samples. This adjustment was made based on the results obtained from rheology experiments
105 conducted prior to the pilot scale trial. The storage modulus (G′), which is an indicator of curd
106 elasticity or stiffness during renneting was measured using a rheometer (TA Instruments, New
107 Castle, DE, USA), as reported in a previous study (Ong, Dagastine, Kentish & Gras, 2012) using
108 the same cheese milk used for the pilot scale cheese making. The gelation time, which is defined
109 as the time when the G′ increased rapidly (Fig. 1b thick arrows), was significantly shorter for
110 milk where $CaCl_2$ was added (~500 s for milk with 100 and 300 mg kg^{-1} calcium addition and
111 950 s for milk without calcium addition). The gel without calcium addition was cut after 45 min
112 of coagulation (2700 s) when the stiffness of the gel was 43 Pa (Fig. 1). The addition of $CaCl_2$
113 (100 or 300 mg kg^{-1}) significantly decreased ($P < 0.05$) the time for the gel to reach a G′ of 43 Pa
114 to ~1750 s (Fig. 1, thin arrows). A shorter coagulation time of 30 min was therefore used for the
115 gel with $CaCl_2$ addition in the pilot scale trial to ensure a similar gel consistency, avoiding the
116 production of curd fines during cutting.

After cutting, the curd was cooked by raising the temperature from 32°C to 38°C in 60 min at a rate of 1°C per 10 min with stirring that gradually increased from 5-45 rpm. After 60 min, the cooking temperature was maintained at 38°C with stirring at 45 rpm until the curds and whey reached the target draining pH. The whey was drained and collected for compositional analysis when the pH reached pH 6.2 (Batches 1-3) or 6.0 (Batches 4-6). The coagulation and cooking times are shown in Table 1. The cooked curd samples were combined into blocks of about 15 cm in height and turned at 15 min intervals while the temperature was maintained at 38°C until the pH of the curds reached pH 5.4. The curd was then milled, 2.5 % (w/w) NaCl added and the curd pressed at 689 kPa overnight.

Another six batches of cheeses were made in a second trial using cheese-milk standardized to the same composition and the same conditions applied in the first trial, giving a total of 12 cheeses for the study. Samples for microscopy analysis were collected after each processing step: after gel formation (immediately prior to cutting), after curd cooking (immediately prior to draining), after curd milling (immediately prior to salting) and after pressing (i.e. the cheese).

2.2. Confocal microscopy and cryo scanning electron microscopy

The gel, curd and cheese samples were prepared for microstructure examination by confocal laser scanning microscopy (CLSM; Leica Microsystems, Heidelberg, Germany) using a method reported previously (Ong, Dagastine, Kentish & Gras, 2010). The sample preparation for cryo scanning electron microscopy (cryo SEM) has also been reported (Ong, Dagastine, Kentish & Gras, 2011). Briefly, samples 5 mm x 2 mm x 2 mm were fixed by rapid plunging into a liquid nitrogen slush (*ca.* -210°C). The fixed sample was then freeze-fractured in a vacuum chamber, etched at -95°C for 30 min, coated with a mixture of gold and palladium and transferred to a cryo stage maintained at –140°C inside the SEM chamber. The sample was observed using a Quanta SEM (Fei, Hillsboro, OR, USA). Two images were taken for each of the six treatments in each of the two independent trials. The images shown are thus representative of the four images obtained for each of the six treatments.

2.3. Image analysis

147 Image analysis and three dimensional image reconstruction were carried out using an
148 Imaris software package (Bitplane, South Windsor, CT, USA). For each 3D image, 40 adjacent
149 planes were recorded; each consisting of 2D layers 512 x 512 pixels in size and the separation
150 between the planes was 0.25 μm. The image analysis was performed following a previously
151 published method (Ong et al., 2012). The porosity of the sample was calculated from the pore
152 volume fraction, assessed from the volume within a sample that was not stained by fat or protein
153 specific dyes, with respect to total volume of the sample. The data presented are the mean of the
154 four images collected for each treatment (n = 4).
155
156 ***2.4. Cheese composition, fat and protein retention and cheese yield***
157 The fat, protein, pH and moisture content of the cheese were determined as described
158 previously (Ong et al., 2012). Fat and protein lost in the whey (FL and PL, respectively) and fat
159 and protein retained in the cheese (FRet and PRet, respectively) were calculated on the basis of
160 the fat or protein concentrations in the cheese-milk. The fat or protein balance (the sum of fat or
161 protein lost in the whey and the fat or protein retained in the cheese), yield of cheese (Ya), dry
162 matter yield of cheese (YDM) were also determined as described in Ong et al. (2012). The
163 cheese yield data are presented as the mean of 2 data points obtained for the two independent
164 trials (n = 2). The fat, protein and moisture content analyses were performed in duplicate for each
165 of the six treatments in each trial. The data presented are the mean of 4 data points collected for
166 the two independent trials (n = 4).
167
168 ***2.5. Texture measurement***
169 A texture analyser (Stable Micro System, Godalming, UK) was used to measure the
170 hardness and cohesiveness of the cheese with conditions described in a previous study (Ong et
171 al., 2012). Texture measurement were repeated six times for each of the six independent samples
172 from each batch of cheese, which were then averaged to give one data point for each treatment in
173 each trial. The results were presented as the average of two means for each treatment from the
174 two independent trials (n = 2).
175
176 ***2.6. Calcium and phosphorus concentrations***

177 Inductively Coupled Plasma Optical Emission Spectroscopy (Varian, Palo Alto, CA,
178 USA) was used to measure the total calcium and phosphorous content as reported previously
179 (Ong et al., 2012). The analysis was performed in duplicate for each of the six treatments in each
180 trial. The data presented are the mean of 4 data points collected for each treatment for the two
181 independent trials (n = 4).
182
183 ***2.7. Statistical analysis***
184 Statistical analysis of the results was carried out using Minitab statistical package
185 (Minitab Inc., State College, PA, USA). A general linear model was used to study the effect of
186 treatments (calcium addition, draining pH and their interactions) with a significance level of α =
187 0.05.
188
189 **3. Results and discussion**
190
191 ***3.1. Variation in cheese making parameters***
192 The addition of $CaCl_2$ and the alteration of the draining pH require changes to the timing
193 of the cheese making process to ensure the process remains consistent with the approach that
194 would be taken in a manufacturing setting. Specifically, the time allocated for ripening of the
195 milk was reduced for samples with additional $CaCl_2$ (Table 1) to ensure that all milk was
196 renneted at ~pH 6.5. A shorter coagulation time of 30 min (Table 1) was used for the gel with
197 $CaCl_2$ addition in the pilot scale trial to ensure a similar gel consistency (G′ of 43 Pa) as
198 indicated in Fig 1. All gels were classified as 'medium set' by an experienced cheese maker prior
199 to cutting. The cooking time of the curd was 30-60 min longer for samples drained at pH 6.0, as
200 compared to pH 6.2. As a result, the addition of $CaCl_2$ shortened the overall processing time
201 when the whey draining pH was 6.2 but was not significantly different (P >0.05) when the
202 draining pH was 6.0 (Table 1). This shorter processing time is desirable, as it allows an increase
203 in plant productivity and a reduction in labour and running costs.
204
205 ***3.2. Microstructure of the gel***
206 The cryo SEM micrographs of the gels (Fig. 2) show a protein network (Pr), which
207 entraps the round fat globules (FG) and starter bacteria (Bc). Some fat globules were dislodged

from the network during freeze-fracture, leaving behind a remnant structure that may be the milk fat globule membrane. Both cryo SEM and CLSM micrographs (Fig. 2) show that the gel made with 300 mg kg^{-1} $CaCl_2$ addition had a denser protein network with smaller pores than the gel without $CaCl_2$ addition. The fat globules were homogeneously distributed within all gels regardless of $CaCl_2$ addition. The 3D image analysis of the gels confirmed the decreased porosity in the gel sample with 300 mg kg^{-1} $CaCl_2$ addition (Table 2). The denser protein network obtained from $CaCl_2$ addition might be expected to mechanically trap more fat globules during whey draining and subsequent processing steps, thus reducing the amount of fat loss during processing. As the gel formed during Cheddar manufacture is somewhat similar to that formed during the production of other cheeses, such as Gouda, these observations may be more widely applicable.

3.3. Microstructure of the cooked curd

During cooking, the fusion of curd particles progressed to a point where a more continuous protein network with smaller pores could be observed (Fig. 3). Several coalesced fat globules (CFG) were also observed as a result of cooking in all samples. The compact structure of the cooked curd makes qualitative comparison of these images harder. The decrease in porosity observed earlier within the gel to which 300 mg kg^{-1} $CaCl_2$ was added could not be observed qualitatively within the cooked curd images. The quantitative analysis of the CLSM images, however, shows the porosity of this cooked curd sample was significantly lower than samples lacking calcium addition at both draining pHs ($P< 0.05$, suppl. Fig. 1a).

It is difficult to see qualitative differences in the number of fat globules from the cryo SEM micrographs of the cooked curd (Fig. 3). Quantitative analysis of the 3D CLSM images shows a significantly higher number of fat globules with added $CaCl_2$ at draining pH of 6.2 ($P < 0.05$, suppl. Fig. 1b). This trend was not evident for $CaCl_2$ addition at draining pH of 6.0, possibly due to the variation in the cooking time (Fig. 1a) required to achieve the target draining pH of 6.0. The large variation observed in the image analysis results also reflects the limitations of this technique; it is difficult to detect differences in a compact curd structure such as what occurs after cooking, where fat coalescence increases and the structure is less homogenous. Compositional analysis of the whey was therefore employed to assess the effect of $CaCl_2$ addition and draining pH on the fat and protein levels in the sample.

3.4. Fat and protein content of the sweet whey

The sweet whey acts as a vehicle that carries the fat dislodged from the curd matrix during cooking and draining. The volume of the whey released was not significantly different ($P > 0.05$) between treatments. The fat concentration within this whey and hence the fat loss was significantly reduced ($P < 0.05$), however, in samples with 300 mg kg^{-1} $CaCl_2$ addition, as compared to the control for both draining pHs (Fig. 4). These results highlight the potential benefit of altering the protein microstructure by means of calcium addition. Interestingly, the denser protein network did not affect the level of protein lost to the sweet whey ($P > 0.05$, Fig. 4). This result was consistent with a previous trial, where it was reported that the non-fat milk solids was not significantly affected for Emmentaler cheese when 100 mg L^{-1} $CaCl_2$ was added (Wolfschoon-Pombo, 1997).

3.5. Microstructure of the milled curd

The microstructure of the curd after cheddaring and milling (Fig. 5) was more compact than the microstructure of the cooked curd (Fig. 4). The cheddaring process involves the fusion of curd particles, particularly once the curd reaches a pH of ~5.8, as a consequence of the loss of Ca and PO_4 from the protein matrix (Lucey & Fox, 1993). Addition of $CaCl_2$ did not affect the microstructure of the milled curd, as observed using cryo SEM or CLSM. The differences in porosity observed within the gel and cooked curd became less evident as the structure became more compact. The draining pH, however, appeared to affect the microstructure of the milled curd.

The continued cheddaring causes the curd to shrink, expelling more moisture. The pore size reduced to approximately 1 μm. These micron size, circular pores were more obvious within the protein strands of milled curds produced at a higher draining pH (Fig. 5a-c) than at a lower draining pH (Fig. 5d-f). Micron size pores have also been observed within the milled curds of samples made using cheese-milk with different milk protein concentrations (Ong, Dagastine, Kentish & Gras, 2013b). These pores were more readily observed within the milled curd made using milk with a lower protein concentration and the final moisture content of the cheese was higher. Such pores may be important in regulating salt retention. The images reinforce that cryo SEM can be used as a tool to capture structural information that can in turn be used to control the

quality of the final cheese product. The bacterial cells also appear in much larger clusters within the milled curd at a draining pH of 6.0 compared to at pH 6.2, possibly due to the longer cooking time for these samples. The difference in distribution was not quantified and the contribution to cheese ripening is unclear and would require further investigation.

Suppl. Fig. 2 provides lower magnification cryo SEM images of the milled curd where curd junctions can be observed. These junctions form when the fat depleted curd fines fuse together during the cheddaring process, forming a protein rich seam within the network. Several crystalline inclusions can be observed especially at curd junctions in samples where 300 mg kg^{-1} $CaCl_2$ had been added at both draining pHs (suppl. Fig. 2a and b). Suppl. Fig. 2 also shows fewer crystalline inclusions at a lower draining pH. The presence of such crystalline phases of salts in the curd and cheese during processing has been reported in several studies (Brooker, 1975; Frau, Mulet, Simal, Massanet & Rossello, 1997). It is not clear, however, if the presence of these crystalline salts relates to calcium lactate formation in cheese and this warrants further investigation.

The micron size pores seen by cryo SEM (Fig. 5) could not be easily observed within the CLSM images (data not shown) due to the presence of the aqueous serum phase and the lower resolution of the CLSM technique. The porosity of the milled curds and the number of fat globules were also not significantly different when assessed by CLSM ($P > 0.05$, suppl. Fig. 1c and d).

3.6. Microstructure and texture of the Cheddar cheese

Pressing reduced the size of the pores observed within the milled curd and the structure became more compact (Fig. 6). The differences between treatments observed at the earlier stages are less obvious at this stage. The 3D CLSM images, however, show the presence of large holes randomly distributed within the cheeses (Fig. 6h, i and j, indicated by the arrows). It is not clear why these holes form. They could be the result of the calcium addition (Ong et al., 2013a) or the longer cooking time and the shorter cheddaring time applied for samples with a lower draining pH, which may prevent the curd from completely fusing together. No clear trend is observed, however, in the porosity of the cheese as a function of pH or calcium addition (suppl. Fig. 1e) suggesting that the distribution of pores is altered rather than the total sample porosity.

Textural analysis of the cheeses indicated that the cheese with a lower draining pH was significantly harder (Fig. 7), possibly due to the lower moisture content of the cheese (Fig. 8a). Addition of $CaCl_2$ up to 300 mg kg^{-1} did not affect the hardness of the cheese ($P > 0.05$). There was also no significant difference in cohesiveness between the treatments ($P > 0.05$) despite the occurrence of holes observed in the cheese, as discussed above. Previous studies have shown that the pH at whey draining influences the texture of a cheese due to changes in the mineral content of the cheese (Lucey & Fox, 1993). Cheeses with a low draining pH, such as Cheshire cheese, are known to be more crumbly than cheese such as Colby, which is drained at a higher pH (Hall & Creamer, 1972). The low draining pH of 6.0 used in this study does not appear to be sufficiently low to cause significant changes to the cohesiveness of the freshly-pressed Cheddar cheese.

3.7. Yield and composition of Cheddar cheese

The fat retained in the cheese was significantly higher with calcium addition at both draining pHs ($P<0.05$, Fig. 8b), possibly due to the lower concentration of fat lost to sweet whey (Fig. 4a). The protein retained in the cheese (Fig. 8b), the yield (Ya) and yield in dry matter (YDM) of the cheeses, however, were not significantly different between treatments ($P>0.05$). The average Ya of the cheeses was 12.2 ± 0.4 % (w/w) and the YDM was 7.9 ± 0.3 % (w/w). Our yield result is in apparent contrast to the findings of Wolfschoon-Pombo (1997) and Ustunol et al. (1990), who both observed an increase in yield of Emmentaler-type cheese or stirred curd cheese, when 100 mg L^{-1} or 200 mg L^{-1} of calcium was added to the cheese-milk. The ~3.5 % difference in fat retention observed in the cheese here is equal to 35 g of increased fat per vat of cheese or increase in yield of ~0.18 % (Ya, estimated as kg cheese per kg of cheese-milk). The variation in Ya observed between the trials conducted here was 0.4 %, which makes the increase in fat retention not observable within the range of variation observed for the Ya data. The total fat and protein mass balance during this cheese making trial was within the range of 94-97% recovery and 90-92% recovery for fat and protein respectively.

The composition of the cheese was within the range usually observed for Cheddar cheese (Fig. 8a, c). There were no significant differences in fat or protein composition with $CaCl_2$ addition ($P >0.05$, Fig. 8c). The concentration of fat and protein in the cheese, however, was significantly higher ($P < 0.05$) in cheeses with a lower draining pH (Fig. 8c) possibly due to the

lower moisture content of these cheeses (Fig. 8a). This is consistent with previously published results, where cheese drained at a lower pH tends to have a lower moisture level (Kiely et al., 1992; Yazici & Akbulut, 2007). The fat in dry matter of the cheeses was not significantly different ($P > 0.05$) regardless of the different treatments (Fig. 8a), showing that moisture was the only significant difference between treatments.

3.8. Total and soluble calcium and phosphorus concentrations

Special whey treatment is normally required if the sweet whey contains an excessive level of calcium but our study shows that the addition of 300 mg kg^{-1} did not change the calcium concentration in the whey and would not necessitate additional treatment. The total calcium in the whey was 346-374 mg kg^{-1} compared to 330-358 mg kg^{-1} for whey from cheese with 300 mg kg^{-1} added $CaCl_2$ vs no added calcium, respectively). Most of the added $CaCl_2$ was retained in the curd. As a result there was an increasing trend in the level of total calcium in the cooked curd and cheese with increasing $CaCl_2$ addition ($P<0.05$) (Fig. 9). The effect of the whey draining pH on the level of the total calcium concentration was more significant, however, than the addition of $CaCl_2$.

More calcium phosphate is solubilised at a lower pH resulting in the higher concentration ($P< 0.05$) of total calcium in the whey (325 ± 24 mg kg^{-1} and 366 ± 8 mg kg^{-1} in whey drained at pH 6.2 or pH 6.0, respectively). As a result, the total calcium retained in the cooked curd and cheese for samples drained at a lower pH was lower regardless of the $CaCl_2$ level (Fig. 9). The difference in the total calcium content of the whey due to the lower draining pH is consistent with a previous study for Cheddar cheese reported by Lucey and Fox (1993).

Fig. 9 also shows an interesting comparison between the different treatments. The level of total calcium in the cheese with a draining pH of 6.2 without added $CaCl_2$ was similar to cheese with a draining pH 6.0 where 300 mg kg^{-1} $CaCl_2$ was added. This suggests the combination of calcium addition and lower draining pH could be used to produce cheese with a similar concentration of calcium to the control (no added $CaCl_2$, pH 6.2). The extra calcium added at the beginning of cheese making would improve coagulation but is drained away by lowering the draining pH. This minimizes potential defects associated with excess calcium in the final cheese, although textural and microstructural analyses show theses cheeses here differ in hardness and the arrangement of pores within the microstructure

The total phosphorus concentration was not affected by the addition of $CaCl_2$. A lower concentration of phosphorus was observed in cheese with a lower draining pH ($P < 0.05$, data not shown), similar to observations for calcium.

4. Conclusion

This study supports evidence from past studies that the addition of calcium chloride has the potential to reduce the fat lost to sweet whey and potentially improve the fat retention in cheese. Advanced microscopy tools such as CLSM and cryo SEM can be used to provide microstructural data to understand the mechanisms of fat retention within the gel during the early stage of cheese making. Quantitative image analysis measures such as porosity, however, are less able to differentiate between the process variables as the curd becomes more compact. The moisture content of the cheese was lower at a lower draining pH and the fat concentration and cheese hardness increased. Chemical and textural analyses were therefore needed in combination with the microstructural data to assess the effect of calcium addition and draining pH.

This study shows that $CaCl_2$ addition in combination with a lower draining pH could be used to improve coagulation at the early stage of cheese making, potentially improving fat retention and maintaining a similar level of total calcium in the final cheese. Our study provides further evidence that the addition of $CaCl_2$ can be used to shorten the processing time and increase factory productivity. Our findings may also be relevant to the manufacture of Gouda type cheeses, which share similar early steps of manufacture with Cheddar cheese.

Acknowledgements

This work was funded by the Australia Research Council (ARC- LP0883300) and Dairy Innovation Australia Limited. LO, SEK and SLG are also supported by the ARC Dairy Innovation Hub (IH120100005). The authors thank the Electron Microscopy Unit and the Biological Optical Microscopy Platform at Bio21 Molecular Science & Biotechnology Institute and the Particulate Fluids Processing Centre, which is a Special Research Centre of the ARC at The University of Melbourne, for equipment access. We also thank Warrnambool Cheese and Butter for their involvement in this project.

392 **References**

393 Brooker, B. E. (1975). Obervations on the microscopic crystalline inclusions in Cheddar cheese.
394 *Journal of Dairy Research, 42*, 341-348.

395 Choi, J., Horne, D. S., Johnson, M. E., & Lucey, J. A. (2008). Effects of the concentration of
396 insoluble calcium phosphate associated with casein micelles on the functionality of
397 directly acidified cheese. *Journal of Dairy Science, 91*, 513-522.

398 Dalgleish, D. G. (1983). Coagulation of renneted bovine casein micelles-dependence on
399 temperature, calcium-ion concentration and ionic strength. *Journal of Dairy Research,*
400 *50*, 331-340.

401 Dalgleish, D. G., & Law, A. J. R. (1989). pH-Induced dissociation of bovine casein micelles. II.
402 Mineral solubilization and its relation to casein release. *Journal of Dairy Research, 56*,
403 727-735.

404 Federal Register (1982). Electronic code of federal regulations. Title 21: Food and Drugs. Part
405 184 - Direct food substances affirmed as generally recognize as safe. Retrieved on 21
406 May 2014. Last updated: 1 April 1996, from www.ecfr.gov.

407 Frau, M., Mulet, A., Simal, S., Massanet, J., & Rossello, C. (1997). Microscopic crystalline
408 inclusions in Mahón cheese / Inclusiones cristalinas microscópicas en el queso Mahón.
409 *Food Science and Technology International, 3*, 43-47.

410 Gastaldi, E., Pellegrini, O., Lagaude, A., & Fuente, B. T. (1994). Functions of added calcium in
411 acid milk coagulation. *Journal of Food science, 59*, 310-312.

412 Guinee, T. P., Feeney, E. P., Auty, M. A. E., & Fox, P. F. (2002). Effect of pH and calcium
413 concentration on some textural and functional properties of mozzarella cheese. *Journal of*
414 *Dairy Science, 85*, 1655-1669.

415 Hall, D. M., & Creamer, L. K. (1972). A study of the sub-microscopic structure of Cheddar,
416 Cheshire and Gouda cheese by electron microscopy. *New Zealand Journal of Dairy*
417 *Science and Technology, 7*, 95.

418 Holmes, D. G., Duersch, J. W., & Ernstrom, C. A. (1977). Distribution of milk clotting enzymes
419 between curd and whey and their survival during Cheddar cheese making. *Journal of*
420 *Dairy Science, 60*, 862-869.

421 Kiely, L. J., Kindstedt, P. S., Hendricks, G. M., Levis, J. E., Yun, J. J., & Barbano, D. M. (1992).
422 Effect of draining pH on the development of curd structure during the manufacture of
423 mozzarella cheese. *Food Structure, 11*, 217-224.
424 Lucey, J. A., & Fox, P. F. (1993). Importance of calcium and phosphate in cheese manufacture: a
425 review. *Journal of Dairy Science, 76*, 1714-1724.
426 Okigbo, L. M., Richardson, G. H., Brown, R. J., & Ernstrom, C. A. (1985). Effects of pH,
427 calcium chloride, and chymosin concentration on coagulation properties of abnormal and
428 normal milk. *Journal of Dairy Science, 68*, 2527-2533.
429 Ong, L., Dagastine, R. R., Kentish, S. E., & Gras, S. L. (2010). The effect of milk processing on
430 the microstructure of the milk fat globule and rennet induced gel observed using confocal
431 laser scanning microscopy. *Journal of Food Science, 75*, E135-E145.
432 Ong, L., Dagastine, R. R., Kentish, S. E., & Gras, S. L. (2011). Microstructure of gel and cheese
433 curd observed using cryo scanning electron microscopy and confocal microscopy. *LWT -*
434 *Food Science and Technology, 44*, 1291-1302.
435 Ong, L., Dagastine, R. R., Kentish, S. E., & Gras, S. L. (2012). The effect of pH at renneting on
436 the microstructure, composition and texture of Cheddar cheese. *Food Research*
437 *International, 48*, 119-130.
438 Ong, L., Dagastine, R. R., Kentish, S. E., & Gras, S. L. (2013a). The effect of calcium chloride
439 addition on the microstructure and composition of Cheddar cheese. *International Dairy*
440 *Journal, 33*, 135-141.
441 Ong, L., Dagastine, R. R., Kentish, S. E., & Gras, S. L. (2013b). Microstructure and composition
442 of full fat Cheddar cheese made with ultrafiltered milk retentate. *Foods, 2*, 310-331.
443 Phadungath, C., & Metzger, L. E. (2011). Effect of sodium gluconate on the solubility of calcium
444 lactate. *Journal of Dairy Science, 94*, 4843-4849.
445 Udabage, P., McKinnon, I. R., & Augustin, M. A. (2001). Effects of mineral salts and calcium
446 chelating agents on the gelation of renneted skin milk. *Journal of Dairy Science, 84*,
447 1569-1575.
448 Ustunol, Z., & Hicks, C. L. (1990). Effect of calcium addition on yield of cheese manufactured
449 with endothia parasitica Protease. *Journal of Dairy Science, 73*, 17-25.
450 Walstra, P., Wouters, T. M., & Geurts, T. J. (2006). Cheese manufacture. In *Dairy Science and*
451 *Technology* 2nd ed., (pp. 583-638). Boca Raton, FL, USA.

452 Wolfschoon-Pombo, A. F. (1997). Influence of calcium chloride addition to milk on the cheese
453 yield. *International Dairy Journal, 7*, 249-254.
454 Yazici, F., & Akbulut, C. (2007). Impact of whey pH at drainage on the physicochemical,
455 sensory and functional properties of mozzarella cheese made from buffalo milk. *Journal*
456 *of Agricultural and Food Chemistry, 55*, 9993-10000.
457 Zoon, P., van Vliet, T., & Walstra, P. (1988). Rheological properties of rennet-induced skim
458 milk gels. 3. The effect of calcium and phosphate. *Netherlands Milk & Dairy Journal, 42*,
459 295-312.

460 **List of Figures**

461

462 **Fig. 1.** The storage modulus (G′) measured from the time of rennet addition for cheese-milk
463 without $CaCl_2$ addition (dotted line), with 100 mg kg^{-1} $CaCl_2$ addition (thin solid line), or with
464 300 mg kg^{-1} $CaCl_2$ addition (thick solid line). The thick arrows indicate the gelation point when
465 G′ reaches ~5 Pa) and the thin arrows indicate the cutting point when G′ reaches 43 Pa. Error
466 bars are the standard deviation of the mean from two independent trials (n = 2).

467

468 **Fig. 2.** Cryo SEM (first row, **a-c**) and CLSM (second row, **d-f** and third row, **g-i**) micrographs of
469 gels made using cheese-milk without $CaCl_2$ addition (left), with 100 mg kg^{-1} $CaCl_2$ addition
470 (middle) or 300 mg kg^{-1} $CaCl_2$ addition (right). FG = fat globules, Pr = protein network and Bc =
471 bacteria. The black areas correspond to pores. The 3D CLSM micrograph (second row) is
472 constructed from 40 layers of 2D images with a total depth of 10 μm. The middle section of the
473 3D protein reconstruction (third row) is presented in three views: the X-Y image (top), X-Z
474 image (bottom) and Z-Y (right). Scale bars within the cryo SEM and CLSM images are 10 μm
475 and 20 μm in length respectively. Nile red stained fat appears red and FCF fast green stained
476 protein appears green. Please refer to the online edition for a colour version of this figure.

477

478 **Fig. 3.** Cryo SEM micrographs of cooked curd made using cheese-milk without $CaCl_2$ addition
479 (**a, d**), with 100 mg kg^{-1} $CaCl_2$ addition (**b, e**) or 300 mg kg^{-1} $CaCl_2$ addition (**c, f**) where the
480 whey was drained at pH 6.2 (**a-c**) or at pH 6.0 (**d-f**). FG = fat globules, CFG = coalesced fat
481 globules, Pr = protein network and Bc = bacteria. The black areas correspond to pores. Scale bars
482 within the cryo SEM images are 10 μm in length.

483

484 **Fig. 4.** The effect of $CaCl_2$ addition on the percentage of fat lost (FL, ■ or □ with solid line) or
485 protein lost (PL, ▲ or Δ with dotted line) to the sweet whey at pH 6.2 (closed markers, ■ or ▲)
486 or pH 6.0 (open markers, □ or Δ). Error bars are the standard error of the mean (n = 4).

487

488 **Fig. 5.** Cryo SEM micrographs of milled curd made using cheese-milk without $CaCl_2$ addition
489 (**a, d**), with 100 mg kg^{-1} $CaCl_2$ addition (**b, e**) or 300 mg kg^{-1} $CaCl_2$ addition (**c, f**) where the
490 whey was drained at pH 6.2 (a-c) or at pH 6.0 (d-f). FG = fat globules, CFG = coalesced fat

491 globules, Pr = protein network, Bc = bacteria and Cr = crystalline inclusion. The black areas
492 correspond to pores. Scale bars within the cryo SEM images are 10 μm in length.
493
494 **Fig. 6.** Cryo SEM micrographs of Cheddar cheese made using cheese-milk without $CaCl_2$
495 addition (**a, d**), with 100 mg kg^{-1} $CaCl_2$ addition (**b, e**) or 300 mg kg^{-1} $CaCl_2$ addition (**c, f**) where
496 the whey was drained at pH 6.2 (**a-c**) or at pH 6.0 (**d-f**). FG = fat globules, CFG = coalesced fat
497 globules, Pr = protein network and Bc = bacteria. The black areas correspond to pores.
498 Representative CLSM micrographs of Cheddar cheese made using cheese-milk without $CaCl_2$
499 addition (**g, i**) or with 300 mg kg^{-1} $CaCl_2$ addition (**h, j**) where the whey was drained at 6.2 (**g, h**)
500 or pH 6.0 (**i, j**). The 3D images each consist of 40 layers of 2D images with a total depth of 10
501 μm. Scale bars within the cryo SEM and CLSM images are 10 μm and 20 μm in length
502 respectively. Nile red stained fat appears red and FCF fast green stained protein appears green.
503 Please refer to the online edition for a colour version of this figure.
504
505 **Fig. 7.** The hardness (■ or □ with dotted line) or and cohesiveness (▲ or Δ with solid line) of
506 Cheddar cheese made with different concentration of $CaCl_2$ addition at a draining pH of 6.2
507 (closed markers, ■ or ▲) or pH 6.0 (open markers, □ or Δ). Error bars are the standard error of
508 the mean (n = 2). Each mean is the average of 6 texture analyses from the same batch of cheese.
509
510 **Fig. 8.** The effect of $CaCl_2$ addition or whey draining pH on **a)** the concentration of moisture in
511 cheese (Moisture, ■ or □ with dotted line) and the fat concentration in dry matter of the cheese
512 (FDM, ▲ or Δ with solid line); **b)** the percentage of fat (FRet, ■ or □ with solid line) or protein
513 retained in the cheese (PRet, ▲ or Δ with dotted line); **c)** the concentration of fat (Fat, ■ or □
514 with solid line) or protein in cheese (Protein, ▲ or Δ with dotted line). The whey draining pH
515 was 6.2 (closed markers, ■ or ▲) or pH 6.0 (open markers, □ or Δ). The fat and protein retained
516 were calculated on the basis of fat and protein concentration in the cheese-milk. Error bars are
517 the standard error of the mean (n = 4).
518
519 **Fig. 9.** The effect of $CaCl_2$ addition or whey draining pH on the level of total calcium in the curd
520 collected after cooking (Cooked, ▲ or Δ with solid line) and after pressing (Cheese, ■ or □ with

dotted line). The whey draining pH was 6.2 (closed markers, ■ or ▲) or pH 6.0 (open markers, □ or Δ). Error bars are the standard error of the mean (n = 4).

Supplementary Fig. 1. Physical properties of the cooked curd (a-b), milled curd (c-d) and cheese (e-f) made with different levels of $CaCl_2$ addition. All properties were determined by three dimensional image analysis of CLSM images. Results are presented as the mean ± the standard error of the mean (n = 4). The whey draining pH was 6.2 (closed marker, ■, ● or ▲ with solid line) or pH 6.0 (open markers, □, ○ or Δ with dotted line).

Supplementary Fig. 2. Cryo SEM micrographs of milled curd made using cheese-milk with 300 mg kg^{-1} $CaCl_2$ addition and with a whey draining pH of 6.2 (a) or pH 6.0 (b). The white circles indicate the presence of crystalline inclusions. Arrows indicate the curd junction. Scale bars within the images are 50 μm in length.

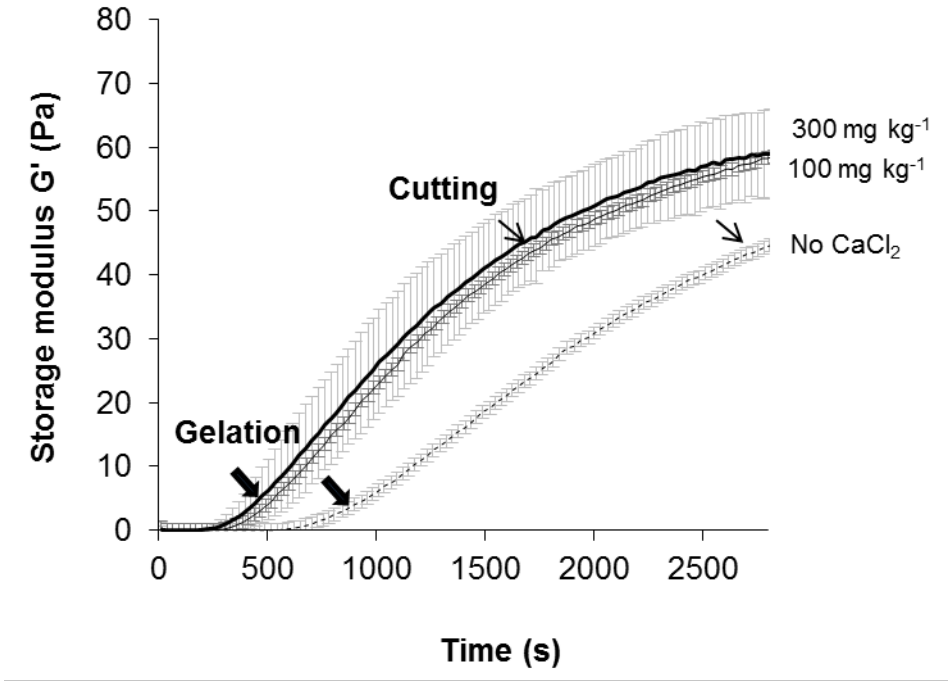

Fig. 1. The storage modulus (G´) measured from the time of rennet addition for cheese-milk without $CaCl_2$ addition (dotted line), with 100 mg kg^{-1} $CaCl_2$ addition (thin solid line), or with 300 mg kg^{-1} $CaCl_2$ addition (thick solid line). The thick arrows indicate the gelation point when G´ reaches ~5 Pa) and the thin arrows indicate the cutting point when G´ reaches 43 Pa. Error bars are the standard deviation of the mean from two independent trials (n = 2).

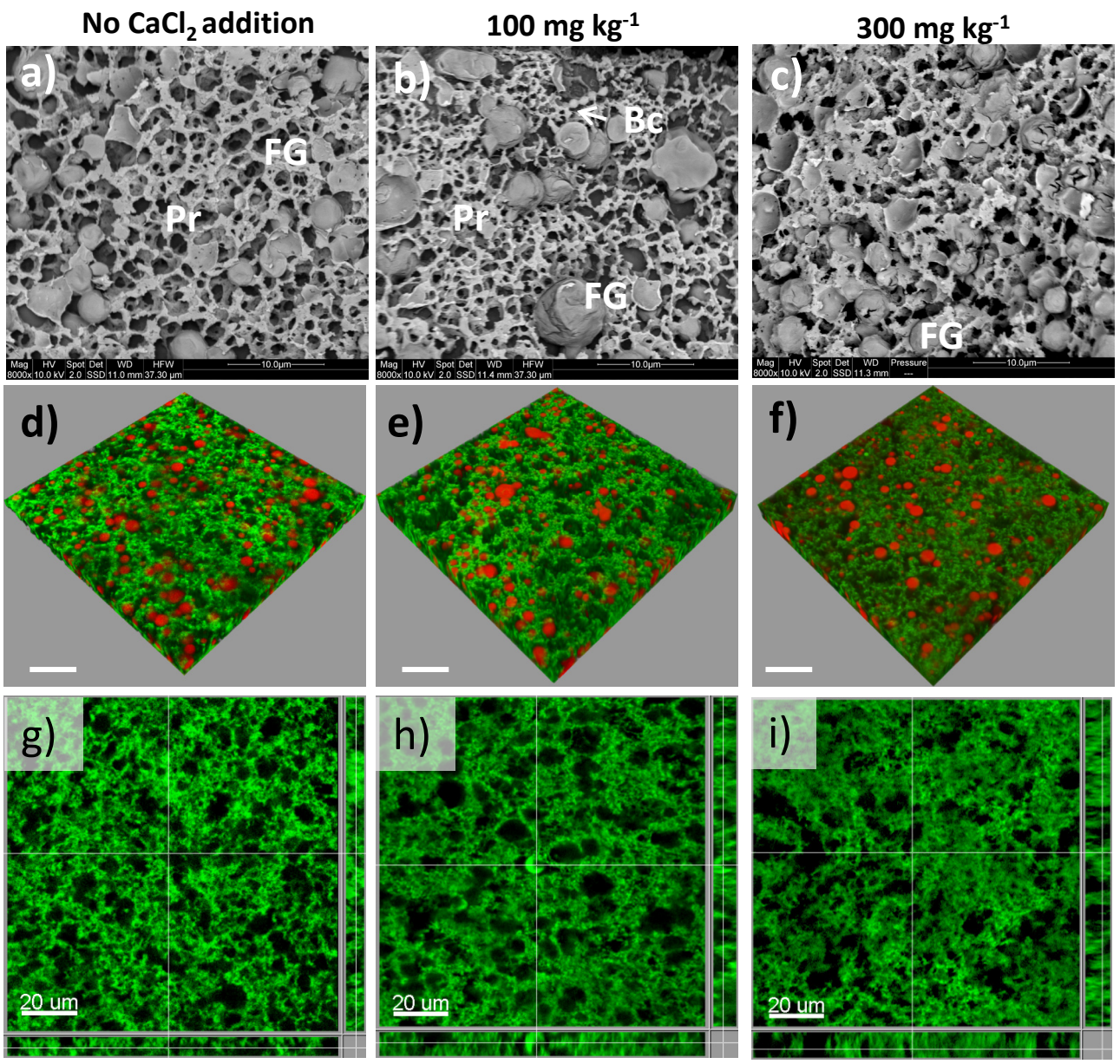

Figure 2. Cryo SEM (first row, **a-c**) and CLSM (second row, **d-f** and third row, **g-i**) micrographs of gels made using cheese-milk without $CaCl_2$ addition (left), with 100 mg kg^{-1} $CaCl_2$ addition (middle) or 300 mg kg^{-1} $CaCl_2$ addition (right). FG = fat globules, Pr = protein network and Bc = bacteria. The black areas correspond to pores. The 3D CLSM micrograph (second row) is constructed from 40 layers of 2D images with a total depth of 10 µm. The middle section of the 3D protein reconstruction (third row) is presented in three views: the X-Y image (top), X-Z image (bottom) and Z-Y (right). Scale bars within the cryo SEM and CLSM images are 10 µm and 20 µm in length respectively. Nile red stained fat appears red and FCF fast green stained protein appears green.

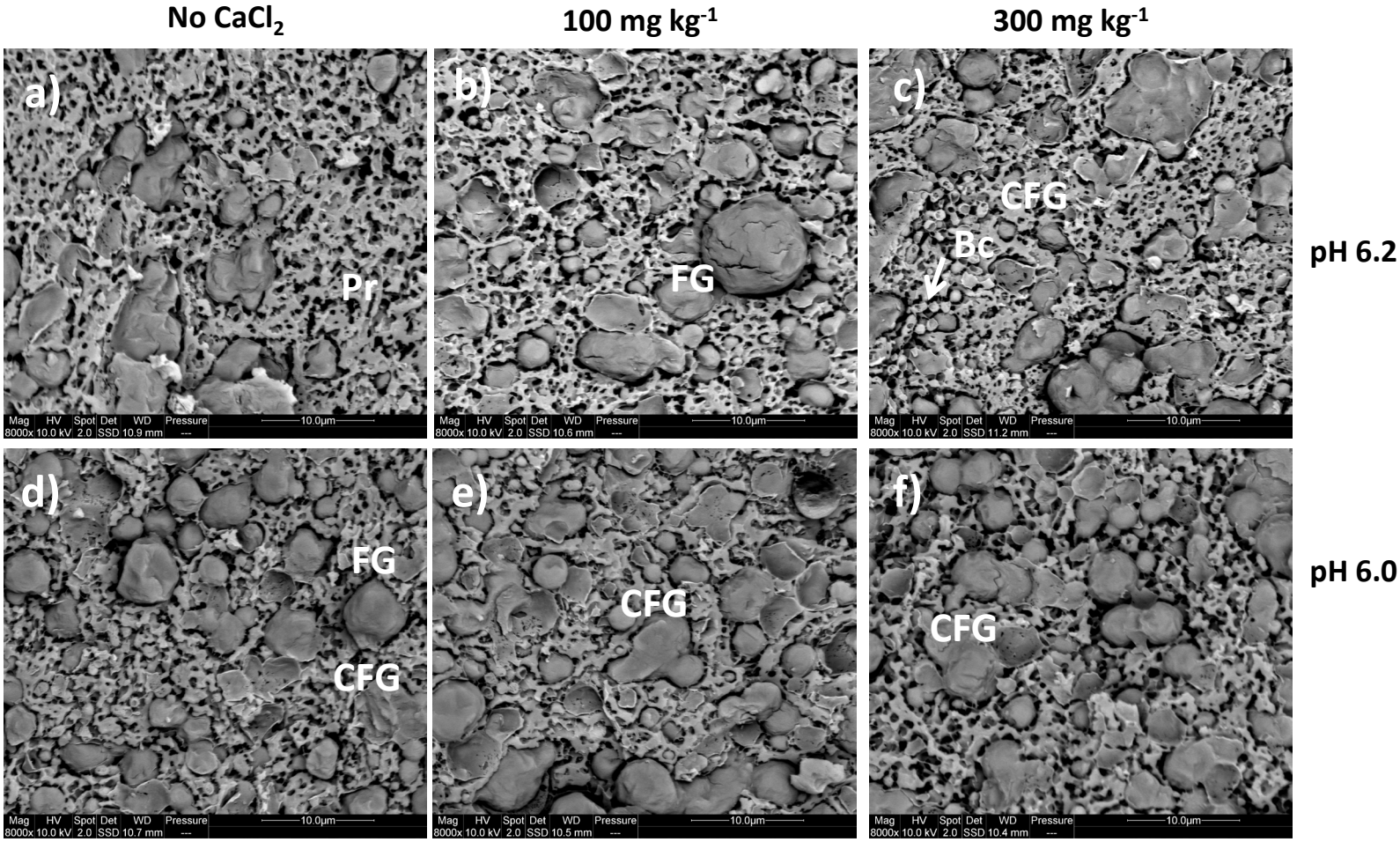

Fig. 3. Cryo SEM micrographs of cooked curd made using cheese-milk without $CaCl_2$ addition (**a, d**), with 100 mg kg^{-1} $CaCl_2$ addition (**b, e**) or 300 mg kg^{-1} $CaCl_2$ addition (**c, f**) where the whey was drained at pH 6.2 (**a-c**) or at pH 6.0 (**d-f**). FG = fat globules, CFG = coalesced fat globules, Pr = protein network and Bc = bacteria. The black areas correspond to pores. Scale bars within the cryo SEM images are 10 µm in length.

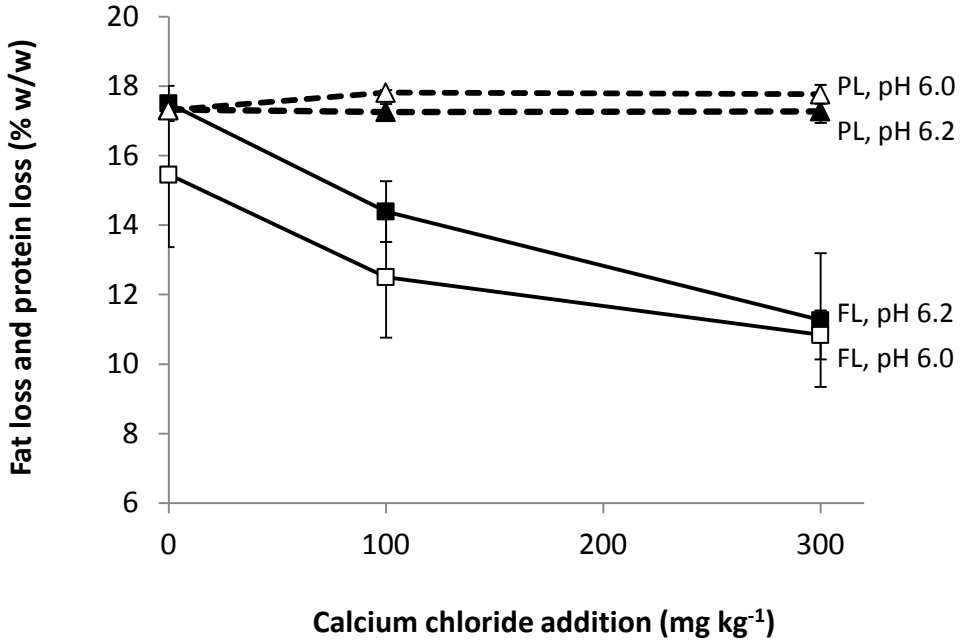

Fig. 4. The effect of $CaCl_2$ addition on the percentage of fat lost (FL, ■ or □ with solid line) or protein lost (PL, ▲ or Δ with dotted line) to the sweet whey at pH 6.2 (closed markers, ■ or ▲) or pH 6.0 (open markers, □ or Δ). Error bars are the standard error of the mean (n = 4).

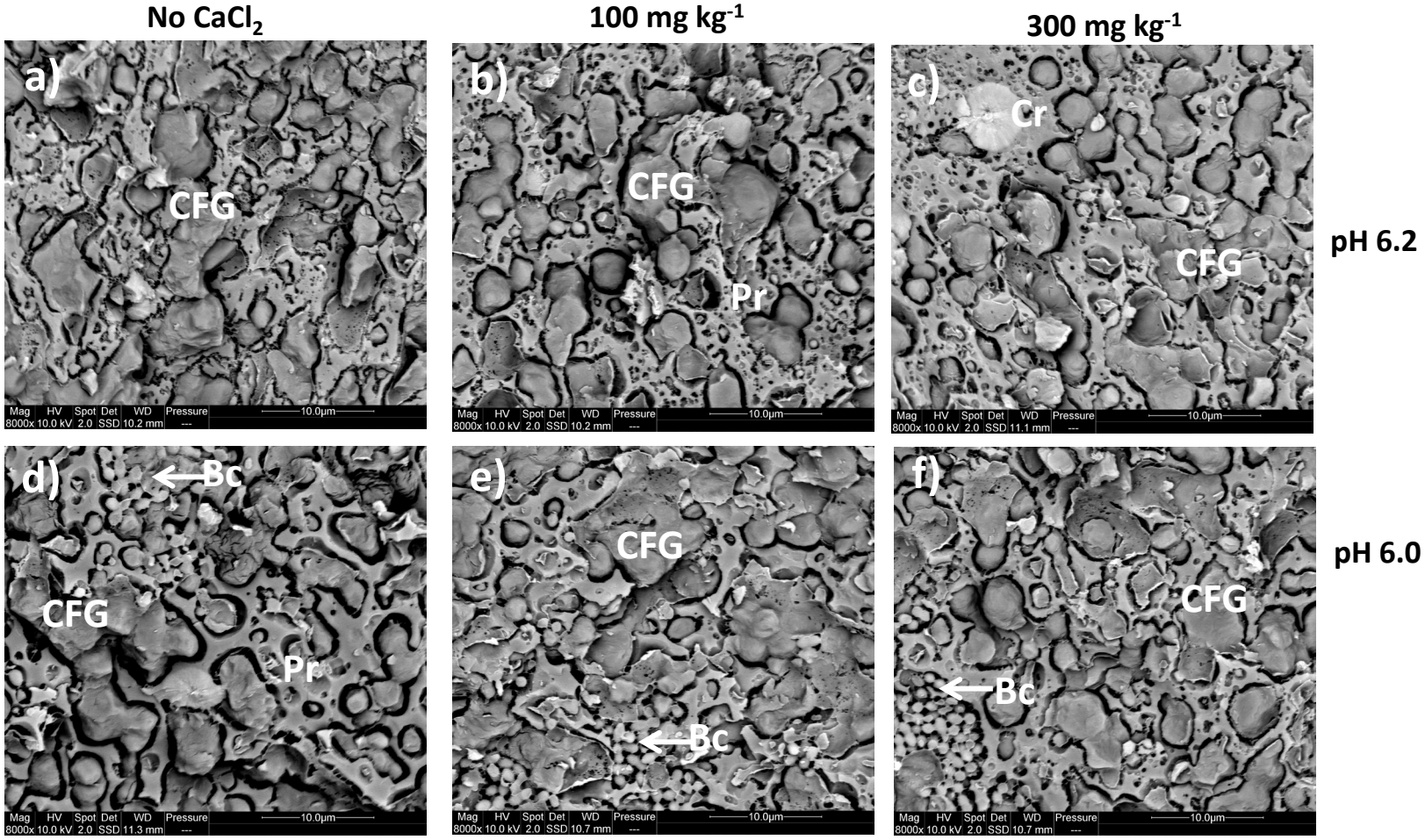

Fig. 5. Cryo SEM micrographs of milled curd made using cheese-milk without $CaCl_2$ addition (**a, d**), with 100 mg kg^{-1} $CaCl_2$ addition (**b, e**) or 300 mg kg^{-1} $CaCl_2$ addition (**c, f**) where the whey was drained at pH 6.2 (**a-c**) or at pH 6.0 (**d-f**). FG = fat globules, CFG = coalesced fat globules, Pr = protein network, Bc = bacteria and Cr = crystalline inclusion. The black areas correspond to pores. Scale bars within the cryo SEM images are 10 µm in length.

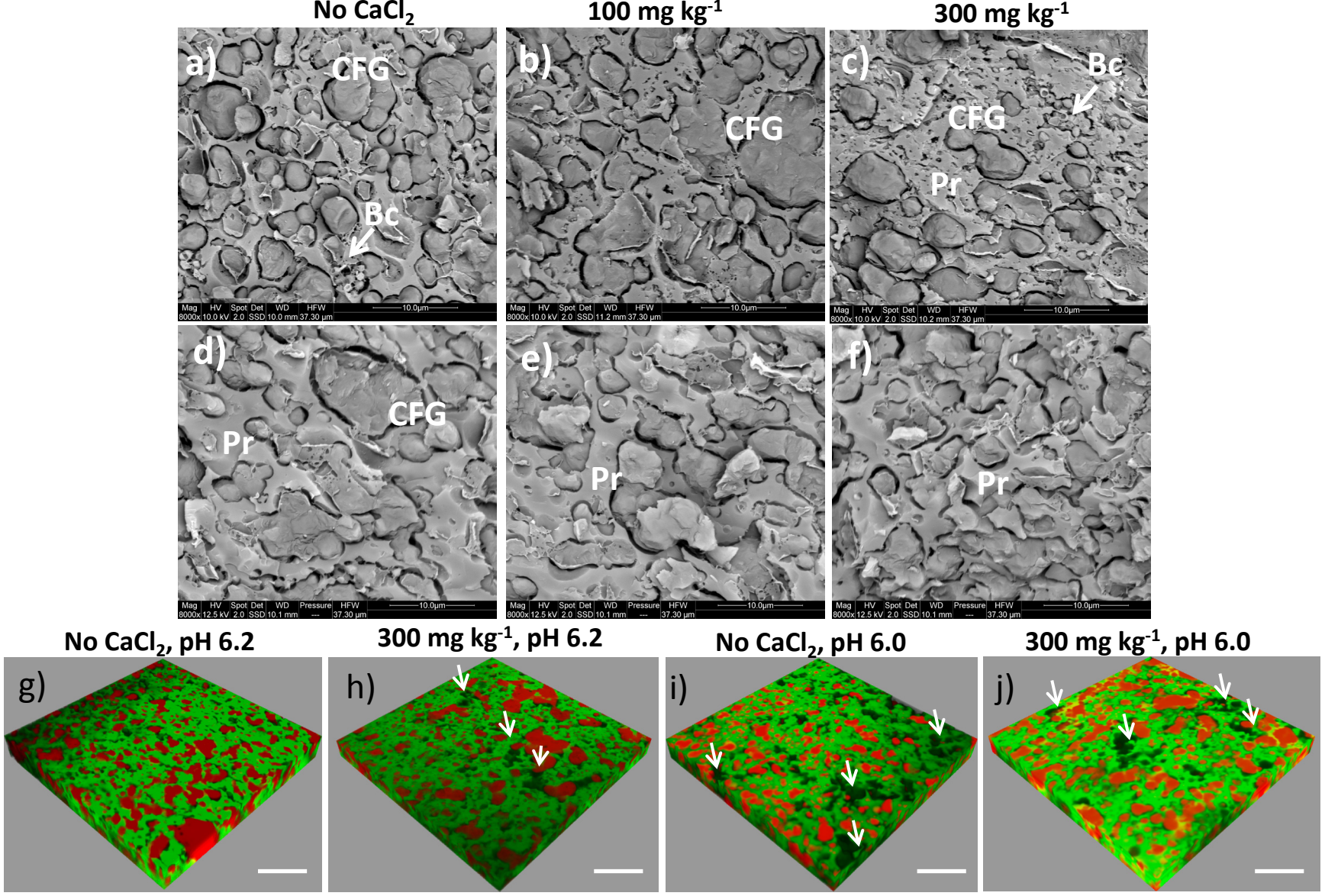

Fig. 6. Cryo SEM micrographs of Cheddar cheese made using cheese-milk without $CaCl_2$ addition (**a, d**), with 100 mg kg^{-1} $CaCl_2$ addition (**b, e**) or 300 mg kg^{-1} $CaCl_2$ addition (**c, f**) where the whey was drained at pH 6.2 (**a-c**) or at pH 6.0 (**d-f**). FG = fat globules, CFG = coalesced fat globules, Pr = protein network and Bc = bacteria. The black areas correspond to pores. Representative CLSM micrographs of Cheddar cheese made using cheese-milk without $CaCl_2$ addition (**g, i**) or with 300 mg kg^{-1} $CaCl_2$ addition (**h, j**) where the whey was drained at 6.2 (**g, h**) or pH 6.0 (**i, j**). The 3D images each consist of 40 layers of 2D images with a total depth of 10 µm. Nile red stained fat appears red and FCF fast green stained protein appears green. Scale bars within the cryo SEM and CLSM images are 10 µm and 20 µm in length respectively.

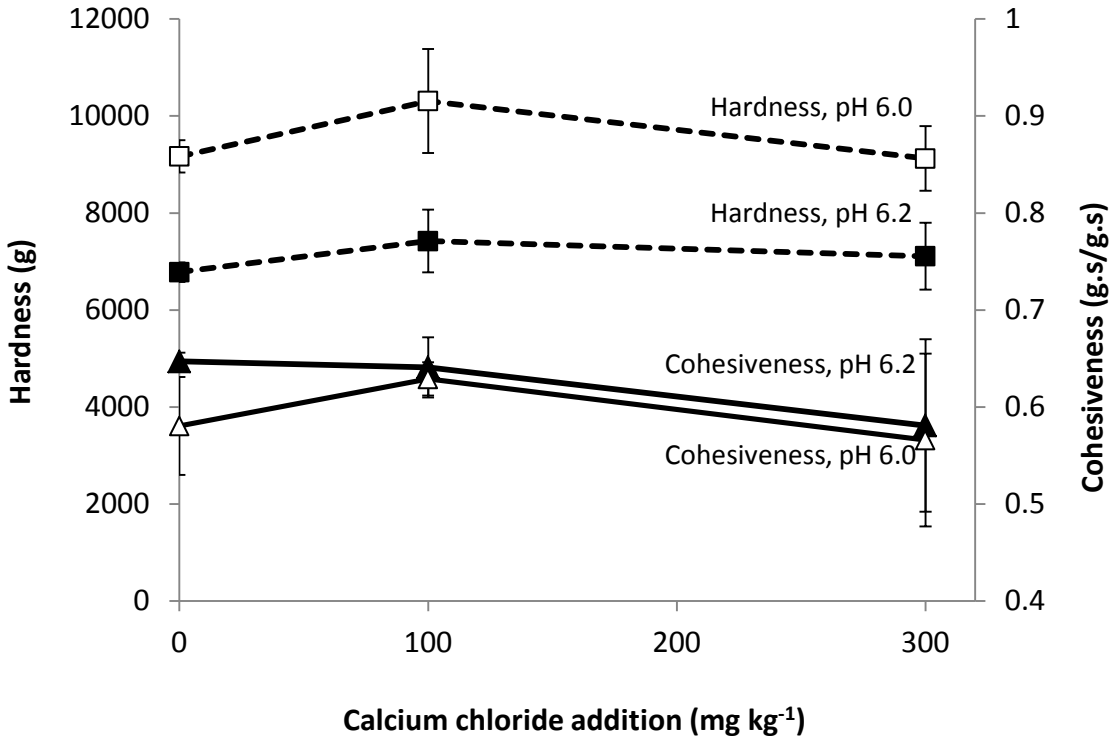

Fig. 7. The hardness (■ or □ with dotted line) or and cohesiveness (▲ or Δ with solid line) of Cheddar cheese made with different concentration of $CaCl_2$ addition at a draining pH of 6.2 (closed markers, ■ or ▲) or pH 6.0 (open markers, □ or Δ). Error bars are the standard error of the mean (n = 2). Each mean is the average of 6 texture analyses from the same batch of cheese.

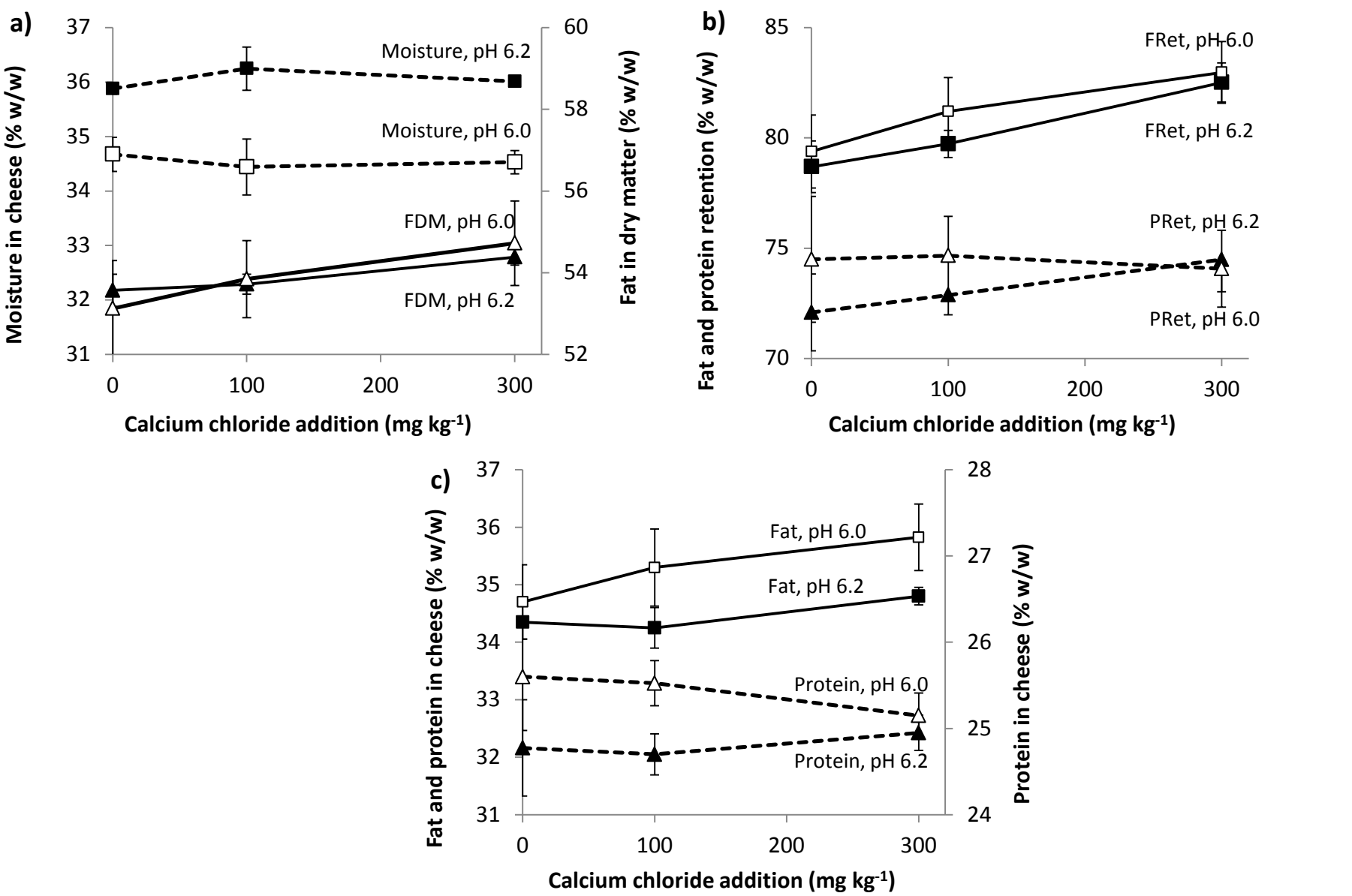

Fig. 8. The effect of $CaCl_2$ addition or whey draining pH on **a)** the concentration of moisture in cheese (Moisture, ■ or □ with dotted line) and the fat concentration in dry matter of the cheese (FDM, ▲ or Δ with solid line); **b)** the percentage of fat (FRet, ■ or □ with solid line) or protein retained in the cheese (PRet, ▲ or Δ with dotted line); **c)** the concentration of fat (Fat, ■ or □ with solid line) or protein in cheese (Protein, ▲ or Δ with dotted line). The whey draining pH was 6.2 (closed markers, ■ or ▲) or pH 6.0 (open markers, □ or Δ). The fat and protein retained were calculated on the basis of fat and protein concentration in the cheese-milk. Error bars are the standard error of the mean (n = 4).

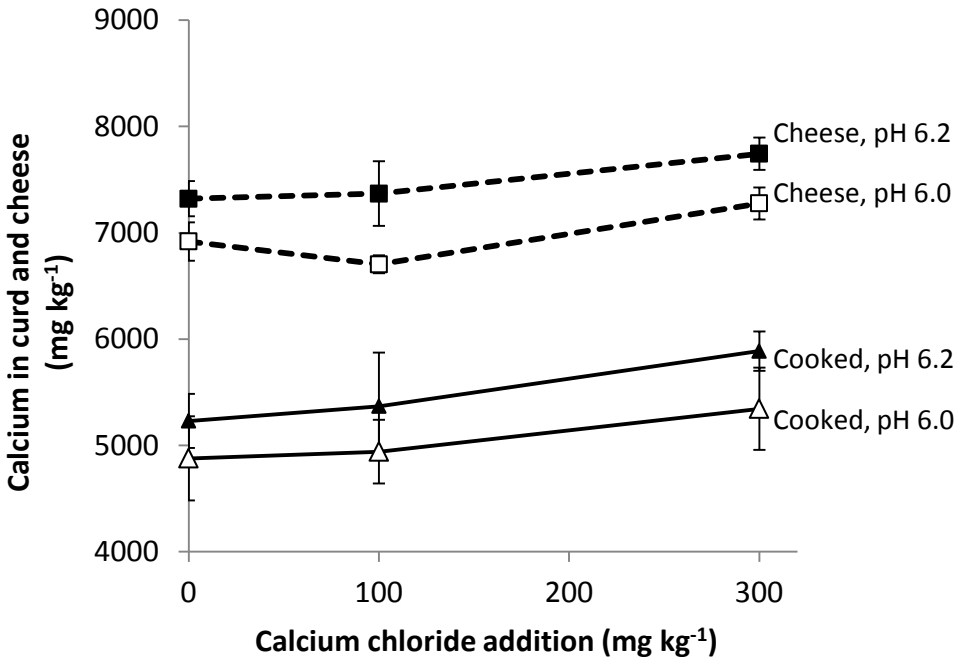

Fig. 9. The effect of $CaCl_2$ addition or whey draining pH on the level of total calcium in the curd collected after cooking (Cooked, ▲ or Δ with solid line) and after pressing (Cheese, ■ or □ with dotted line). The whey draining pH was 6.2 (closed markers, ■ or ▲) or pH 6.0 (open markers, □ or Δ). Error bars are the standard error of the mean (n = 4).

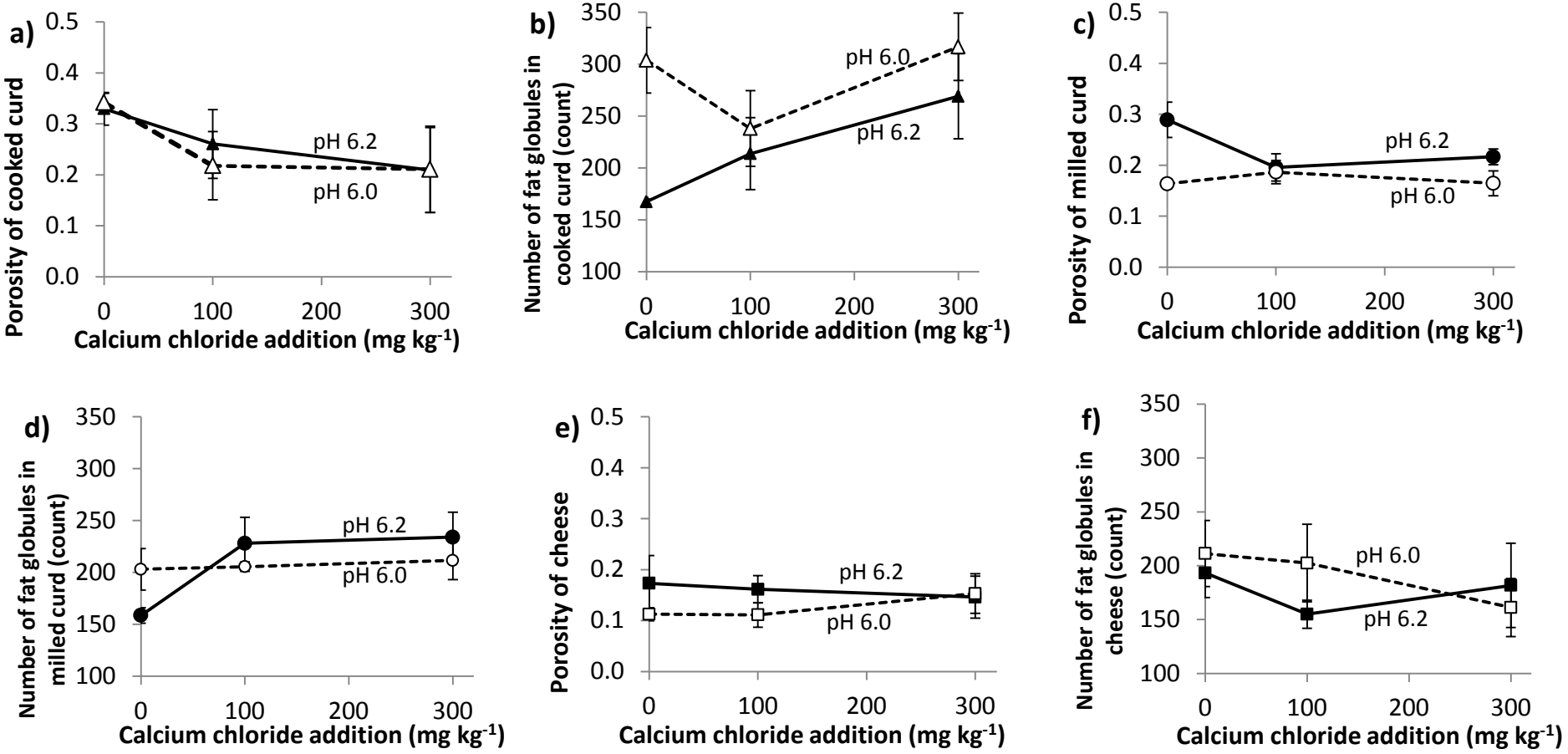

Supplementary Fig. 1. Physical properties of the cooked curd (**a-b**), milled curd (**c-d**) and cheese (e-f) made with different levels of $CaCl_2$ addition. All properties were determined by three dimensional image analysis of CLSM images. Results are presented as the mean ± the standard error of the mean (n = 4). The whey draining pH was 6.2 (closed marker, ■, ● or ▲ with solid line) or pH 6.0 (open markers, □, ○ or Δ with dotted line).

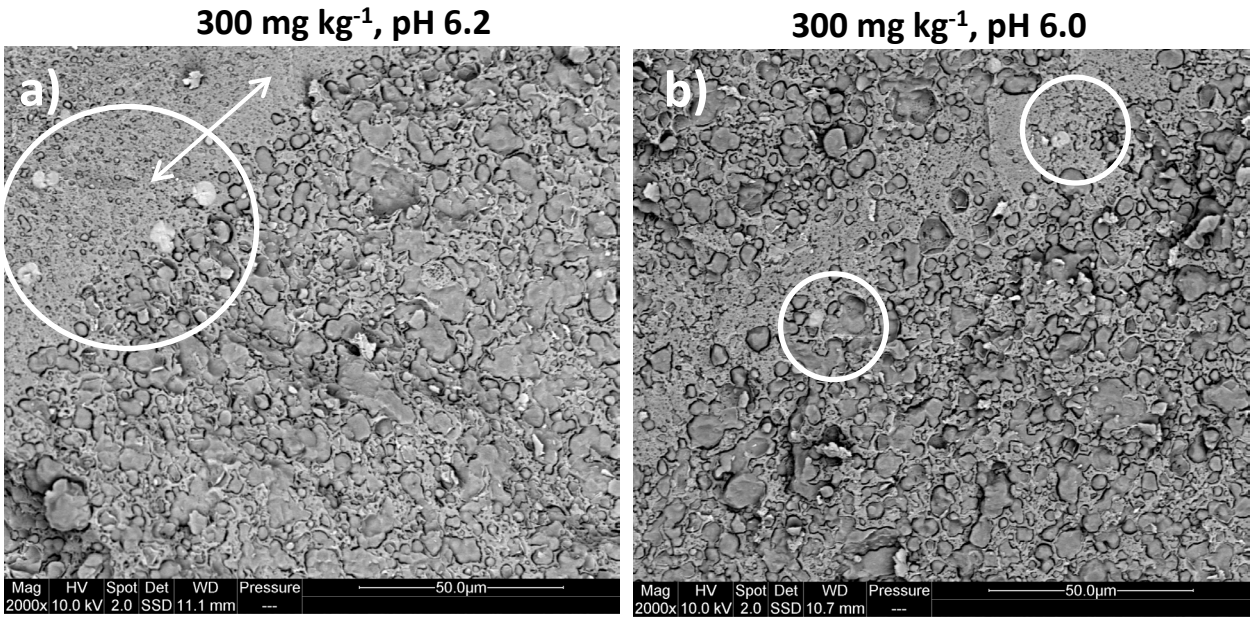

Supplementary Fig. 2. Cryo SEM micrographs of milled curd made using cheese-milk with 300 mg kg^{-1} $CaCl_2$ addition and with a whey draining pH of 6.2 (**a**) or pH 6.0 (**b**). The white circles indicate the presence of crystalline inclusions. Arrows indicate the curd junction. Scale bars within the images are 50 µm in length.